Carbon anodes for a lithium secondary battery based on polyacrylonitrile

Yuping Wu [a,b,*], Shibi Fang [b], Yingyan Jiang [b]

[a] *Institute of Nuclear Energy Technology, Tsinghua University, Beijing, 102201, China*
[b] *Institute of Chemistry, Chinese Academy of Sciences, Beijing, 100080, China*

Abstract

Carbon anode materials for a lithium secondary battery based on polyacrylonitrile (PAN) are studied by using elemental analysis, X-ray powder diffraction, scanning electron microscopy and X-ray photoelectron spectroscopy. The reversible lithium capacity and charging voltage curves of carbons from PAN are affected by the heat-treatment temperature the rate of temperature rise and the soak time. These factors lead to a change in nitrogen content, cyclization and cross-linking processes, the carbon structure, and the number of micropores. The reversible capacity reaches 426 mAh g^{-1} at 600°C; the lower the rate of temperature rise, the higher the reversible capacity. The addition of phosphoric acid can favour the cyclization process of PAN, and can increase the number of micropores in the resulting carbon. It can also act as setting agent for graphene molecules and can improve the regularity of the carbon structure. In addition, the doped phosphorus is bonded with C and O, and dispersed homogeneously in the bulk carbon structure. This results in an increase in d_{002}. Such doping can enhance the reversible capacity above and below 0.9 V. © 1998 Elsevier Science S.A. All rights reserved.

Keywords: Lithium secondary battery; Carbon anodes; PAN; Phosphoric acid

1. Introduction

Since the commercialization of the lithium–ion secondary battery in the early 1990s, many types of graphitized carbonaceous materials have been investigated as negative electrodes, e.g., pitch, coke, carbon fibre. These carbons require high-temperature (> 2000°C) treatment and their reversible capacities are limited compared with lithium metal (i.e., lower than 372 mAh g^{-1}). Thus, many candidate materials have been studied in order to lower the cost and improve the properties of lithium secondary batteries. These materials include polymeric carbons [1], $Li_{3-x}M_xN$ (M: transitional metal elements such as Co, Ni, Cu, Fe and Mn) [2], and tin-based composite oxides [3]. Polymeric carbon is regarded as an ideal anode material for the next generation of lithium secondary batteries [4] because its preparation is less critical than that of graphitized carbon (it requires low temperature, < 1000°C) and its reversible capacity is very high (> 372 mAh g^{-1}).

Carbon fibres based on polyacrylonitrile (PAN), such as M-46 obtained at high temperature, have been studied as negative electrodes for lithium secondary batteries [5–7]. They can be used but their reversible capacity is generally not higher than 300 mAh g^{-1}. This suggests that polymeric carbons from PAN may be more promising electrode materials.

In this paper, an examination is made of the properties of carbons from PAN at temperatures below 1000°C and the effect of heat-treatment condition is investigated. In addition, the influence of phosphoric acid addition is studied.

2. Experimental

A 30-ml sample of monomer acrylonitrile (AN), purified by distillation, was put in a 3-neck flask with 120-ml dimethyl formamide (DMF) and then stirred. After adding 0.3 wt.% initiator azo-*bis*-isobutyronitrile (AIBN), the polymerization was conducted at 60°C for 8 h. The solution was then cast into a plate and dried under vacuum. The resulting thin film was used for the preparation of

* Corresponding author. Tel.: +86-10-6977−13−50; Fax: +86-10-6977−14−64

carbon under argon atmosphere in a tube furnace as reported previously [8]. The carbon product was powdered through a 320-mesh sieve.

Elemental analysis was performed by means of the Heratus CHN-rapid method. X-ray powder diffraction (XRD) data were obtained with a D/MAX-3B instrument and scanning electron micrographs (SEM) were obtained with a Hitachi S530 spectrometer. In order to increase the contrast of the micrographs, all carbon samples were pre-coated with a thin layer of gold. X-ray photoelectron spectra (XPS) were collected on a ES300 instrument of Karatos; the X-ray source was MgKα.

The capacity of the carbonaceous materials was measured with lithium metal as both the counter and the reference electrode. The negative electrode was prepared from 10 mg of the carbonaceous material with 5 wt.% PVDF (4 wt.% solution in NMP) as a binder. The electrolyte was 1-M LiPF$_6$ dissolved in the mixture of DEC and EC (volume ratio 3:7). The discharge and charge voltages were between 2.0 and -0.03 V and the electric current density was 0.20 mA cm^{-2}. The cut-off voltage of discharge was -0.03 V [8].

Phosphoric acid was introduced into the powdered PAN film and mixed for 20 min. After reaction at 100°C for 2.5 h, the mixture was pyrolyzed and analyzed by means of the above procedure.

3. Results and discussion

3.1. Carbon anode from pure PAN

3.1.1. Effect of heat-treatment temperature

The elemental analysis of the carbons obtained at different heat-treatment temperatures is given in Table 1. The data show that the contents of interatoms such as N and H decrease with the temperature. At high temperatures, the interatoms are thermodynamically unstable in the carbon structure and are released as gases such as HCN and CH$_4$ [9]; thus, the contents of interatoms are decreased.

The X-ray powder diffraction pattern of the above carbons are shown in Fig. 1. Only the diffraction peak for the 002 plane is clear while the other peaks, viz., 100, 101, are indeterminate. This suggests that this kind of carbon is
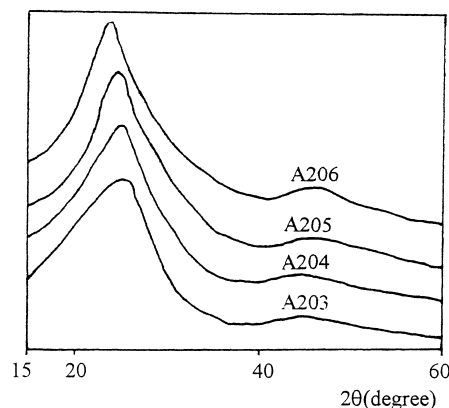

Fig. 1. X-ray powder diffraction patterns for carbons obtained from pure PAN at different heat-treatment temperatures.

amorphous, and consists of graphite crystallites and disordered areas. The distance between the 002 planes, d_{002}, is about 3.5 Å. The width of the 002 peaks becomes narrower with the temperature, that is, the size of the graphite crystallites becomes slightly larger, as can be seen from the data in Table 1.

The charging curves of the carbon anodes obtained at different temperatures are given in Fig. 2. It can be seen that the reversible lithium capacity first increases with temperature and then decreases when the temperature reaches 600°C. In addition, the charging voltages decrease with the temperature. It is well known that PAN molecules can form a carbon structure only when the temperature is above 500°C [9]. Below 500°C, the main processes are the cyclization of PAN molecules and the cross-linking between cyclized PAN molecules [9]. When the heat-treatment temperature increases, the carbonization process proceeds more completely and, therefore, this affects the size of the graphite crystallites to provide effective lithium intercalation [10]. The existence of nitrogen can affect the reversible capacity [11,12], viz., the higher the content of nitrogen, the higher the reversible capacity. Further, the heat-treatment condition affects the number of micropores, which are also effective places for lithium storage [13,14].

When the heat-treated polymer has no carbon structure, it will not act effectively as a host material for lithium storage and the reversible capacity will be very low, even

Table 1

Elemental analysis and X-ray powder diffraction of polymeric carbons obtained from pure PAN at 0.5°C/min and a soak time of 150 min with different heat-treatment temperatures

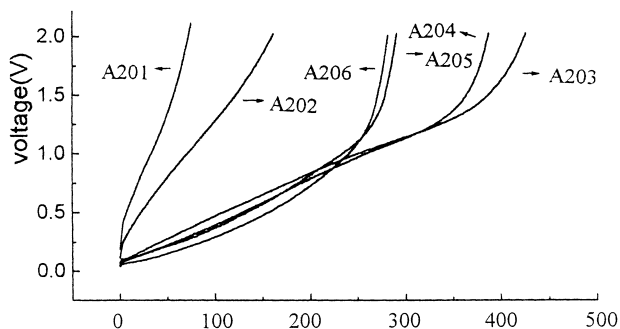| Sample	Temperature (°C)	Ratio of H/C	Ratio of N/C	d_{002} (Å)	Crystal size L_c (Å)
A201	400	0.503	0.263	–	–
A202	500	0.425	0.229	–	–
A203	600	0.351	0.178	3.520	11.41
A204	700	0.323	0.122	3.552	11.85
A205	800	0.217	0.113	3.559	12.07
A206	900	0.155	0.017	3.602	12.89

Fig. 2. Charging voltage curves for carbon anodes obtained from pure PAN at different heat-treatment temperatures.

though the number of micropores is not negligible [15]. With amorphous carbon, the disordered areas have large numbers of micropores, and lithium deintercalates from these places at a voltage higher than 0.9 V [13]. Lithium deintercalates from graphite crystallites at a voltage higher than 0.9 V [13]. Since the size of the graphite crystallites increases with the temperature, the charging voltage decreases with temperature. The combined effects of nitrogen, the size of the graphite crystallites and the number of micropores result in the highest reversible capacity being achieved at 600°C. If there is no nitrogen, the highest capacity will be at a higher temperature, such as 700°C [10].

3.1.2. Effect of the rate of temperature rise

The charging voltage curves of carbon anodes, heat-treated at 600°C obtained at different rates of temperature are presented in Fig. 3. The data show that the lower the rate, the higher the reversible capacity and the lower the charging voltage. It is well known that the processes of cyclization and cross-linking will proceed more completely when the temperature is raised more slowly, thus the carbonization process will be favoured. During the heat-treatment, more vacancies left by the evolved small molecules can be kept in the formed product and will

result in an increase in the micropores. Therefore, in Fig. 3, the reversible capacity above and below 0.9 V increases.

3.1.3. Effect of soak time during heat-treatment

During heat-treatment, the soak time will affect the properties of the obtained carbons. It will affect the carbon structure, though not much because the temperature is well below 2000°C (800°C). By contrast, the micropores will change with soak time. Some micropores are produced by the release of gases such as HCN and CH_4 and some micropores in the carbon structure can coalesce and disappear. This will result in a decrease in micropores when the time becomes longer. These two processes will lead to a maximum number of micropores. The number of micropores affects the reversible capacity above 0.9 V. The charging voltage curves of carbon obtained at 800°C under different soak times are given in Fig. 4. The reversible capacity is highest at a time of 150 min, which is consistent with the above results.

This kind of polymeric carbon is different from that reported previously [16], which was also obtained by pyrolyzing PAN at low temperature. Due to the large amounts of inorganic or organic salts that are added to the precursor, the specific surface area is increased markedly and the pores left by rinsing out the salts may be sufficiently large to act effectively as places for the intercalation of anions such as ClO_4^- [16].

3.2. Carbon anode from PAN added with phosphoric acid

3.2.1. Effect of H_3PO_4 addition on the content and bondage state of nitrogen

Elemental analysis results listed in Table 2 show that the content of nitrogen is almost unchanged at 600°C. Fig. 5 gives the X-ray photoelectron binding energy spectra of nitrogen N_{1s} in carbons obtained from heat-treatment at 600°C and with or without phosphoric acid addition. The spectra show that the nitrogen consists of two kinds [12], namely, graphene nitrogen and conjugated nitrogen, which
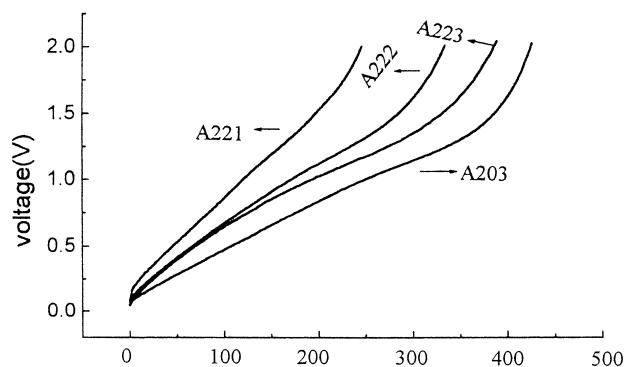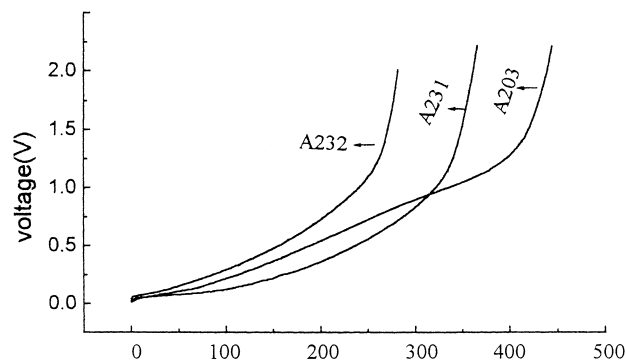

Fig. 3. Charging voltage curves for carbon anodes obtained at different temperature rise rates under heat-treatment at 600°C and a soak time of 150 min (A221 5.0°C/min; A222 2.5°C/min; A223 1.0°C/min; A203 0.5°C/min).

Fig. 4. Charging voltage curves for carbon anodes obtained at different soak times, t, under heat-treatment at 600°C and rising rate of temperature of 0.5°C/min (A231 $t = 60$ min; A203 $t = 150$ min; A232 $t = 600$ min).

Table 2
Elemental analysis and X-ray powder diffraction of polymeric carbons obtained from PAN with H_3PO_4 at 5°C/min and a soak time of 150 min

Sample	Temperature (°C)	Amount of added H_3PO_4 (wt.%)	Ratio of N/C	d_{002} (Å)	Crystal size L_c (Å)
A221	600	0.0	0.202	3.510	9.62
B231	600	5.0	0.204	3.536	10.06
B232	600	10.0	0.196	3.547	11.12
B233	600	20.0	0.206	3.633	10.30

correspond to a binding energy at 398.2 and 400.1 eV, respectively. Although there is only a slight change in the position of the binding energy, the content of graphene nitrogen is increased from 46.5 to 51.8 wt.% and that of conjugated nitrogen is decreased from 53.5 to 48.2 wt.%. Because acid can initiate the cyclization process [17], the added H_3PO_4 can enhance the process and more graphene structure can be obtained.

3.2.2. Effect of H_3PO_4 addition on carbon structure

The X-ray powder diffraction profiles of the carbons obtained at 600°C after the addition of H_3PO_4 are shown in Fig. 6, and summarized in Table 2. The interlayer distance, d_{002}, increases after the addition of H_3PO_4. The 002 peaks become narrower and the graphite crystallite size is increased. The H_3PO_4 can react with the side –CN groups in PAN molecules to form a cross-linked structure, and this cross-linking favours the carbonization process. Although the acid favours the carbonization, the phosphorus atom is larger than the carbon atom (1.06 vs. 0.77 Å), and phosphorus bonds with C and O and is dispersed homogeneously in the bulk carbon structure, thus the interlayer distance d_{002} is increased.

3.2.3. Effect of H_3PO_4 addition on carbon morphology

Scanning electron micrographs (SEM) of carbons obtained by heat-treatment at 600°C are presented in Fig. 7. These micrographs show that the carbon from pure PAN is
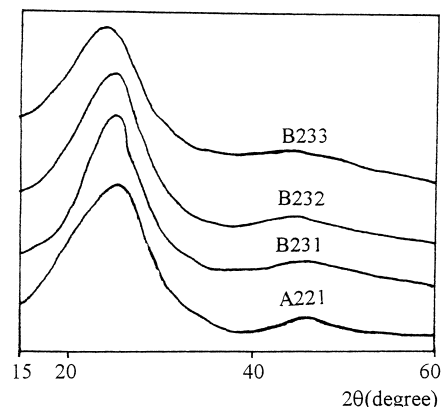

Fig. 6. X-ray powder diffraction patterns for carbons obtained from pure PAN or PAN with phosphoric acid under heat-treatment at 600°C.

turbostratic and that with the addition of H_3PO_4 consists of a layer-like structure. This means that H_3PO_4 causes the graphite crystallite to be organized in more regular fashion. The acid bonds with the –CN group of the PAN molecule, and this acts as a setting agent during the carbonization so that the graphene molecules formed during the heat-treatment are more ordered. This effect may be different to that associated with the addition of transitional metal elements such as NiO and CoO [18] and V_2O_5 [8,19] to the carbon precursor. It is suggested that V_2O_5 forms a complex of VO(graphene)$_2$, which acts as nucleation agent for graphite and promotes a layer-like structure [19].
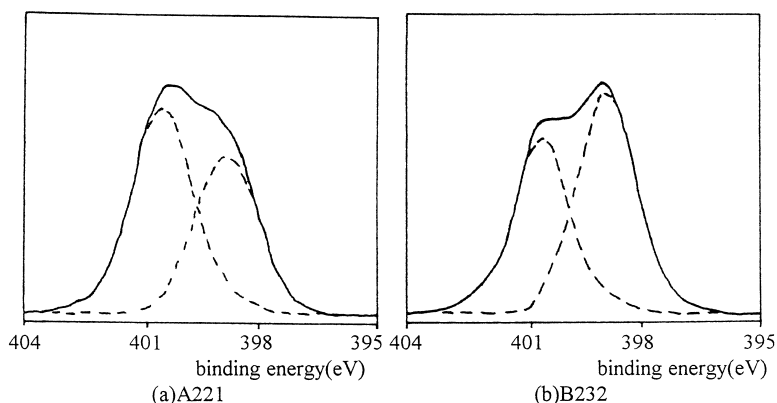

Fig. 5. X-ray photoelectron binding energy spectra for nitrogen N_{1s} in carbons from (a) pure PAN and (b) PAN with 10.0 wt.% phosphoric acid under heat-treatment at 600°C.
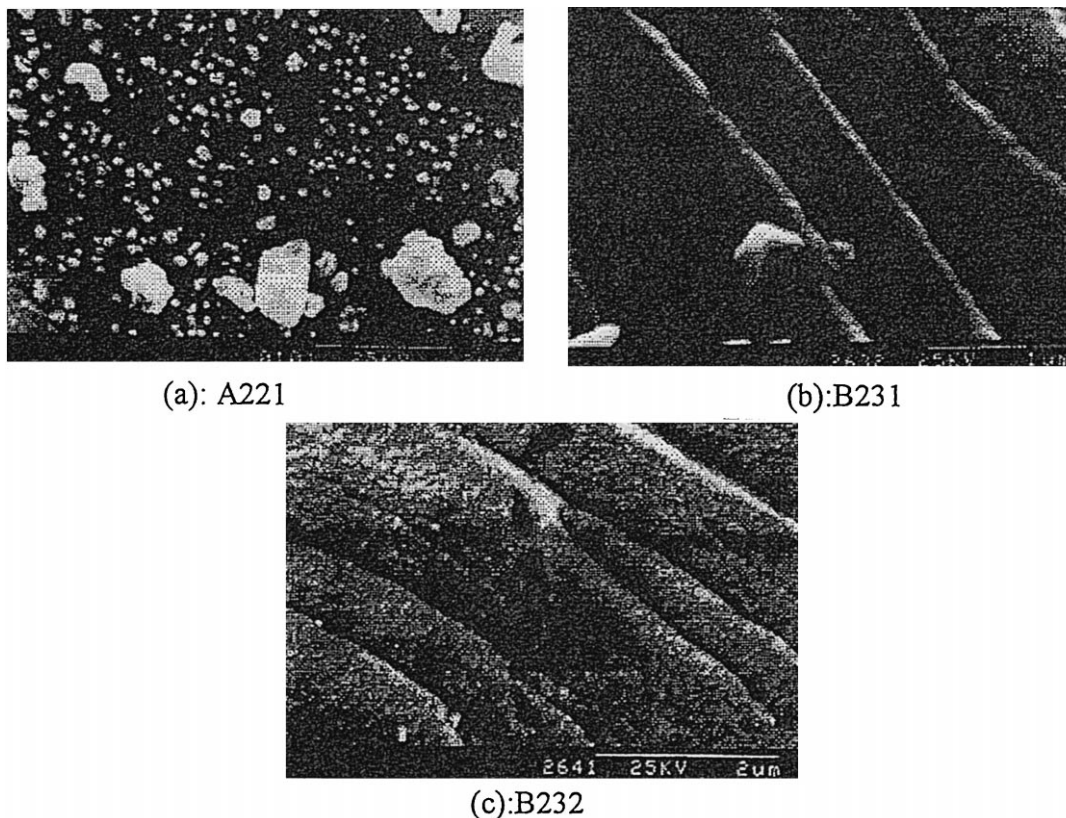
(a): A221   (b): B231

(c): B232

Fig. 7. Scanning electron micrographs of carbons obtained from pure PAN or PAN with H_3PO_4 under heat-treatment at 600°C.

In Fig. 7, some pores in the carbon after the addition of H_3PO_4 can be seen clearly. This is consistent with the results of other authors [20,21]. Phosphoric acid is usually added to prepare activated carbon, which has a large amount of micropores. Pores of size less than 100 nm cannot be detected in scanning electron micrographs.

3.2.4. Bondage of phosphorus to carbon

The X-ray photoelectron binding energy spectrum of P_{2p} in carbon after the addition of H_3PO_4 is shown in Fig. 8. The binding energy of P_{2p} is about 133.7 eV and is near
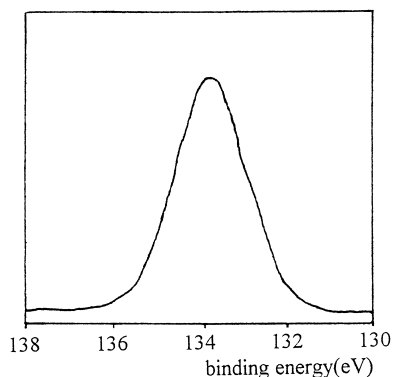
to that of P_{2p} in Ph_3PO, and thus indicates that the introduced P bonds with both carbon and oxygen, i.e., similar to that in carbon obtained from furan resin with H_3PO_4 [22]. The phosphorus is dispersed homogeneously in the bulk structure of carbonaceous materials after heat-treatment at 100°C for some time, which is different from that reported elsewhere [23]. The latter suggested that the phosphorus atoms are deposited on the surface of the carbonaceous material at the edge–plane sites, and thus may serve to expand the layer planes at the surface of the particles and facilitate the intercalation of lithium. In our
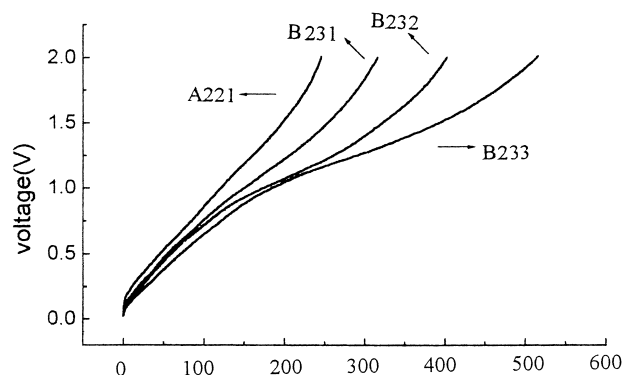

Fig. 8. X-ray photoelectron binding energy spectrum of P_{2p} in the carbon with 10.0 wt.% H_3PO_4.

Fig. 9. Charging voltage curves for carbons obtained from pure PAN or PAN with H_3PO_4 under heat-treatment at 600°C.

results, however, the P in the carbon bulk acts not only at the surface, but also in the bulk.

3.2.5. Effect of H_3PO_4 on reversible capacity

As shown above, the added H_3PO_4 can affect the bondage state of nitrogen, and can also increase the carbonization process and the number of micropores. Concomitantly, the regularity of the carbon structure is increased. Furthermore, phosphorous is doped into the carbon bulk structure and the interlayer distance, d_{002}, is increased. Obviously, these features will lead to a change in the reversible capacity. The charging voltage curves for carbons obtained at 600°C are shown in Fig. 9. The main change is situated at a voltage above 0.9 V and increases with the amount of added H_3PO_4. The reversible capacity below 0.9 V also increases.

4. Conclusions

The heat-treatment conditions such as temperature, rate of temperature rise and soak time can affect the content of N and H, the carbonization process (i.e., the content of graphite crystallites) and the number of micropores in the carbon structure. By virtue of these effects, the reversible lithium capacity is highest at 600°C and increases with slowing down of the rate of temperature rise. The reversible capacity is highest at a specific soak time.

Addition of H_3PO_4 can favour the cyclization process, and result in more graphene nitrogen structure and an increase in graphite crystallite size. In addition, the number of micropores that can act as reservoirs for lithium storage is increased. Further, the H_3PO_4 acts as a setting agent during the heat-treatment and improves the regularity of the carbon structure. The added P bonds with C and O, and is dispersed homogeneously in the carbon. This doping increases the interlayer distance d_{002}. All these factors result in a reversible capacity below and above 0.9 V that increases with the amount of added H_3PO_4.

The behaviour of H_3PO_4 addition changes with carbon precursors. But one fact is clear, namely, doped P can favour the enhancement of the reversible lithium capacity of the obtained carbon anode.

Acknowledgements

References

[1] K. Sato, M. Noguchi, A. Demachi, N. Oki, M. Endo, Science 264 (1994) 556.
[2] T. Shidai, S. Okada, S. Tobishima, J. Yamaki, Solid State Ionics 86–88 (1996) 785.
[3] Y. Idota, T. Kubota, A. Matsufuji, Y. Maekawa, T. Miyasaka, Science 276 (1997) 1395.
[4] S. Yata, Denki Kagaku oyobi Kogyo Butsuri Kagaku 65 (1997) 706.
[5] T. Kitamura, T. Miyazaki, T. Kawagoe, T. Kita, T. Matsunaga, Synth. Met. 18 (1987) 537.
[6] B. Simon, J.P. Boeuve, M. Broussely, J. Power Sources 43–44 (1993) 65.
[7] N. Imanishi, S. Ohashi, T. Ichikawa, Y. Takeda, O. Yamamoto, R. Kanno, J. Power Sources 39 (1992) 185.
[8] Y.P. Wu, S.B. Fang, W.G. Ju, Y.Y. Jiang, J. Power Sources 70 (1998) 114.
[9] K. Jobst, L. Sawtschenko, M. Schwarzenberg, L. Wuckel, Synth. Met. 41–43 (1991) 959.
[10] B. Huang, Y. Huang, Z. Wang, L. Chen, R. Xue, F. Wang, J. Power Sources 58 (1996) 231.
[11] S. Ito, T. Murata, M. Hasegawa, Y. Bito, Y. Toyoguchi, Denki Kagaku oyobi Kogyo Butsuri Kagaku 64 (1996) 1180.
[12] Y.P. Wu, S.B. Fang, Y.Y. Jiang, Solid State Ionics, in press.
[13] A. Mabuchi, T. Katsuhisa, H. Fujimoto, T. Kasuh, J. Electrochem. Soc. 142 (1995) 1041.
[14] G. Sandi, R.E. Winans, K.A. Carrado, J. Electrochem. Soc. 143 (1996) L95.
[15] Y.P. Wu, S.B. Fang, Y.Y. Jiang, J. Mater. Chem., in press.
[16] K. Jobst, L. Sawtschenko, M. Schwarzenberg, G. Paasch, Synth. Met. 47 (1992) 297.
[17] N. Grassie, I.C. McNeil, J. Polym. Soc. 39 (1959) 211.
[18] X. Song, X. Chu, K. Kinoshita, Materials for electrochemical and conversion batteries, capacitors and fuel cells, Mater. Res. Soc. Proc. 393 (1995) 321.
[19] Y.P. Wu, S.B. Fang, Y.Y. Jiang, J. Power Sources, in press.
[20] H.E. Rodes, G. Apai, Mater. Res. Soc. Symp. Proc. 82 (1987) 103, Charact. Def. Mater.
[21] M.M. Sabio, F.R. Reinoso, F. Caturla, M.J. Selles, Carbon 34 (1996) 457.
[22] A. Omura, Proc.-Electrochem. Soc., 93–24, Proceeding of the symposium on lithium batteries, p. 21.
[23] T.D. Tran, J.H. Feikert, X. Song, K. Kinoshita, J. Electrochem. Soc. 142 (1995) 3297.